ABSTRACT

CHANDRA ABHISHEK: Method of lines solution of Richards' equation with spatially and temporally adaptive discretization techniques
(Under the Direction of Cass T. Miller)

Efficient, robust simulation of groundwater flow in the unsaturated zone remains difficult for problems characterized by sharp fronts in both space and time. Employing uniform spatial and temporal discretizations for the numerical solution of these problems can lead to inefficient and expensive simulations. In this work, we solve Richards' equation using the method of lines with both temporally and spatially adaptive approximations. The time discretization adapts both the approximation order and step-size based on formal error control to satisfy user-specified error tolerances. For the spatial discretization, we use h-refinement with a Lagrangian prediction of the fluid front location to determine when and where to refine. We evaluate our method in comparison with uniform spatial discretizations for several test problems. The numerical results demonstrate that this method provides a robust and efficient alternative to standard approaches for simulating variably saturated flow.

Notation

Roman Letters

K_s	saturated hydraulic conductivity
K_z	q effective hydraulic conductivity
S_e	effective saturation, $S_e = (\theta_a - \theta_r)/(\theta_s - \theta_r)$
c	specific moisture capacity $c = d\theta/d\psi$
g	gravity
k_r	relative permeability
m_v	parameter for p-s-k relationship
n_v	parameter for p-s-k relationship
p	pressure
q	macroscopic aqueous phase velocity
t	time coordinate
$\vec{y}$	variable for DAE formulation
$\mathbf{y}'$	temporal derivative for DAE formulation
$\mathbf{y}'_p$	FLCBDF predictor value for $\mathbf{y}'$ in DAE formulation

Greek Letters

Δt	time step
Δt_{adapt}	time step for adaptation
Δz	spatial increment in z direction
$\Delta \mathbf{y}$	Newton increment for DAE formulation
Ω	physical domain
α	FLCBDF coefficient
α_v	parameter for p-s-k relationship
β	water compressibility

β^n	FLCBDF history term
ϵ	absolute error
ϵ_a	absolute tolerance for DAE integrator
ϵ_r	relative tolerance for DAE integrator
θ	volume fraction
θ_r	residual volumetric water content
θ_s	saturated volumetric water content
ρ	density
$\hat{\rho}$	normalized density, $\hat{\rho} = \rho/\rho_0$
ψ	pressure head
ψ^b	Dirichlet boundary value
ψ^0	initial condition for ψ

Abbreviations

BDF	backward difference formula
CPU	elapsed central processing unit time
CR	constant recharge - test problem
DAE	differential algebraic equation
FLCBDF	fixed leading coefficient backward difference formulas
FUNC	number of function evaluations
IVP	initial value problem
JACS	number of jacobian evaluations
LoA	level of adaptation
MOL	method of lines
ODE	ordinary differential equations
PDE	partial differential equations
RE	Richards' equation
RRR	region requiring refinement
STEPS	number of steps taken
SVI	simple vertical infiltration - test problem
VIR	vertical infiltration with redistribution - test problem
p − s − k	pressure-saturation-relative permeability constitutive relations

ACKNOWLEDGMENTS

I would like to take this opportunity to thank my advisor Prof. Cass T. Miller, for his guidance and encouragement through my graduate studies.

I would also like to thank Dr. DiGiano for his role as a teacher and for his valuable suggestions that helped in improving the quality of this report.

I am very grateful to Matthew Farthing and I thank him for his support and guidance. I am thankful to Chris Kees for his valuable advice. Thanks to all the members of the environmental modeling center, Rajah Augustinraj, Doris Pan, Ian Nienhueser, Joe Kanney, Lara Kees, Joe Pedit, Markus Hilpert.

Most of all, I thank my parents, my brother and my sister for their love and for everything they have done for me.

CONTENTS

LIST OF TABLES

LIST OF FIGURES

Chapter 1

Introduction

Efficient and reliable methods for numerically modeling fluid flow in variably saturated porous media are of interest for a number of fields including civil, hydrological and environmental engineering. Often, Richards' Equation (RE) is used to model fluid movement in variably saturated media, [24]. RE is a simplified version of the full two phase system where the air pressure is assumed constant and is obtained by coupling of the aqueous phase mass balance equation with Darcy's law and is closed by constitutive relations to describe the relationship among fluid pressure, saturations, and relative permeabilities [51, 37].

Over the years, a large number of papers have been published on the solution of RE. The most common spatial discretizations have been low order fixed-grid finite difference approaches [17, 12, 11, 35], finite volume methods [49, 29], and finite element approaches [25, 28, 12, 27, 16]. Unfortunately, these methods often require excessively high computational costs to obtain highly accurate solutions for many problems of interest. The nonlinear nature of RE leads to sharp fronts for certain boundary conditions and p-s-k (pressure, saturation and permeability) relations. Under these circumstances uniform-grid solution techniques often require extremely fine temporal and spatial discretizations in order to obtain results of acceptable accuracy. This leads to large CPU times and computer memory requirements. Furthermore, convergence may even be difficult to obtain

under some conditions. For these reasons, we seek alternative approaches for solving RE that are more efficient and more robust.

Adaptive methods seek computational efficiency by using known information about the solution to maximize accuracy while minimizing computational work [4]. Here, we consider a method which combines both temporal and spatial adaption to solve RE for problems characterized by sharp fronts. The temporal approximation is based on a method of lines (MOL) approach that has demonstrated success for modeling variably saturated flow under a number of conditions [30]. We extend this approach to include a spatially adaptive discretization using h refinement.

The objectives of this work are: (1) to formulate a discretization of RE that is variable in both space and time; (2) to outline a method of h-type spatial adaptation implemented in the MOL framework; and (3) then to perform several numerical experiments and compare the space-time adaptation with a uniform spatial discretization.

Chapter 2

Background

2.1 Unsaturated Zone Hydrology

The unsaturated zone (also known as the Vadose zone) is the region above the water table where soil pores are only partially filled with water, and the rest of the pore space is filled with the gaseous phase. Figure 2.1 is a simple sketch that shows the unsaturated zone and the rest of the groundwater distribution. As is very evident from the picture, any pollutant at the surface of the Earth has to pass through the unsaturated zone before it leaches down to the water table or the aquifer. The rate of flow of the aqueous phase in this region is typically very slow, thus the contaminant stays in this region for a long period of time. The unsaturated zone, therefore plays an important and sometimes governing role in the transportation of contaminants in the subsurface.

To be able to model the transport of the contaminants, we need to know very precisely the flow pattern of water, whish is the medium of transportation, this leads us to the need of modeling groundwater flow in the unsaturated zone. In the past, not much attention has been paid on the unsaturated zone as compared to the saturated zone. But now we have started to realize the importance of studying the unsaturated zone, for properly monitoring the contaminant transport in the groundwater.

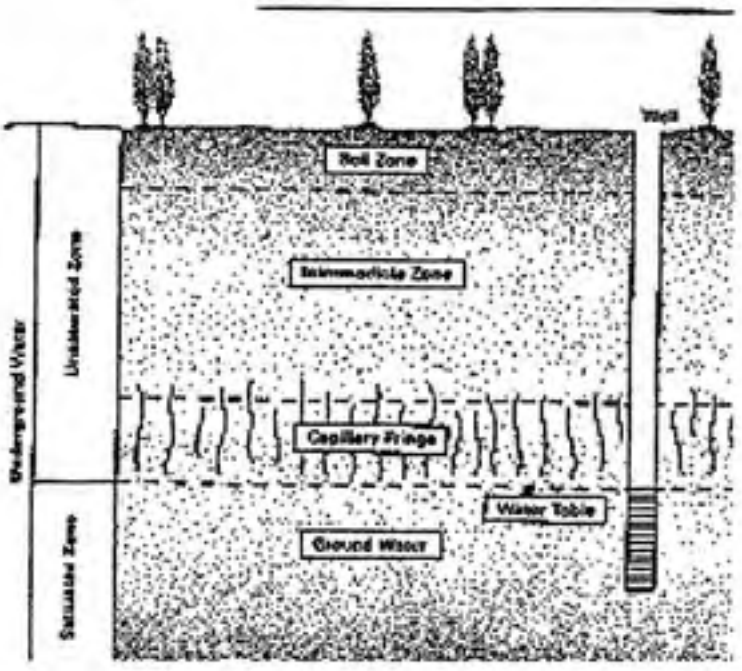

Figure 2.1: Unsaturated Zone.

The major driving force that causes the flow of groundwater in the unsaturated zone is the gravity and the difference in the partial pressures of the aqueous phase and the difference in saturation. The relation between saturation and permeability, an exponential function, is such that the relative permeability takes a value close to 1 when the soil is saturated and is close to 0 at low saturation. Thus, when there is a source of water at the surface of the ground, the region close to the surface becomes saturated and its relative permeability becomes almost 1. If the soil is initially dry, the permeability is negligible elsewhere. This causes a sharp infiltration starting at the boundary and gives rise to a steep front. This front moves ahead with time, maintaining it's steep shape. This steep front and the nonlinear inter-dependence among pressure, saturation and permeability makes unsaturated groundwater flow an interesting but difficult problem to solve.

Many mathematical models have been proposed to simulate the flow of ground-

water in the unsaturated zone, but among them RE is the most popular model. For most of the unsaturated zone flow problems, the auxiliary conditions are such that an analytical solution is not possible, thus we resort to the numerical solution methods. In this chapter we discuss RE and the various numerical methods applied to solve it in the past.

2.2 General Numerical Solution Considerations

2.2.1 Standard forms of RE

RE can be formulated in a number of ways depending on the choice of independent and dependent solution variables [24, 36, 12]. These include the θ-based form, where the volumetric water content (θ) is the independent variable; the ψ-based form in which the pressure-head (ψ) is the solution variable; and the mixed form which is formulated in terms of both θ and ψ. Each of the above three forms of RE has its strengths and weaknesses [22, 12]. The θ based form of RE has the advantage of being inherently mass conservative, but it is not useful in cases where saturation is reached, since the diffusivity term approaches infinity [21]. In addition, θ is not continuous across the interfaces of porous media having different physical properties. The ψ-based form avoids these difficulties and is valid for both unsaturated and saturated conditions. However, it can produce large mass balance errors for solutions with low temporal accuracy [12, 42]. The mixed form of RE is valid for the full range of saturation and is mass conservative, but the fact that it involves two independent variables with only one mass balance equation complicates its numerical solution. For this reason, the methods applied to the mixed form have largely been low order [12, 42, 48].

2.2.2 Numerical methods for solving RE

Having decided the form of RE and the closure relationships, we need a numerical approximation method to solve it. There are a variety of numerical methods described in the literature. Traditionally, numerical solutions to RE have been carried out on a fixed grid using either low-order finite differences method [17, 12, 11, 35], finite volume methods [49, 29] or finite element method [25, 28, 12, 27, 16].

The standard approach when solving RE with finite difference method typically involves backward Euler or Crank-Nicolson time discretization techniques. These methods generally either use a fixed time-step or a time-step adaptation technique based on an empirical strategy. These methods, when applied to the ψ-based form of RE, lead to significant mass balance errors [12]. These mass balance errors can be overcome by applying low-order time discretizations or empirical time-step adaptation strategy to the mixed form of RE, but it has been shown that they are not as efficient as higher order, adaptive MOL discretization of the pressure head form of RE [35, 48].

The constitutive relationships are inherently non-linear in nature. Thus, a system of equations generated by any numerical solution of RE is non-linear. The time integration methods used for RE are usually implicit, so the solution of non-linear systems is of significant importance when solving RE. In the majority of cases iterative techniques like Picard [24, 12] or Newton method [44, 48, 49] have been used. In the past, these non-linearities have also been resolved using non-iterative techniques such as predictor-corrector methods [43]. A comparison of Picard iteration method, Newton iteration method and other non-linear solution techniques is given by [40].

2.3 Adaptive Methods

2.3.1 Temporal adaptation

The time step-size required to meet the desired level of accuracy need not be same at each point in time for the entire simulation. Thus, temporally adaptive methods increase the time step-size at various points, achieving the same level of accuracy, but reducing the total simulation time and thus increasing the efficiency of the simulation. Temporal adaptation has often been achieved in two ways: (1) increasing/decreasing the time step by a constant factor at every time level when changes in the dependent variable (ψ, θ, etc.) are below some tolerance level, [3, 33], or (2) Increasing/decreasing the time step-size based on the number of iterations required to achieve convergence in a Picard or Newton iterative scheme, [1, 33]. Elkadi and Ling [14] have presented an alternate technique for estimating temporal and spatial temporal step-size based on the Peclet and Courant numbers.

Temporal adaptation need not always be done empirically. Approaches based on formal error control have, in fact, demonstrated significant advantages over empirically based adaption strategies [29, 19, 48]. For example, Kavetski et al. [29] have presented a new mathematically based adaptive time stepping technique with embedded error control applied to the mixed form of RE. The method of lines (MOL) is another approach to the solution of time-dependent PDE (partial differential equations) that has shown considerable success for solving multiphase flow problems like RE [19, 48, 35, 49, 30, 53]. The MOL proceeds formally in two steps [46]:

1. Spatial derivatives are approximated. Finite difference or finite element techniques can be used for spatial discretization.

2. The resulting system of semi-discrete (discrete in space and continuous in time) ordinary differential equations (ODEs) or Differential Algebraic

Equations (DAEs) is integrated in time.

The advantage of using the MOL approach is that temporal accuracy can be specified by the user; therefore the error checking, order selection and time-step adaptivity features available in sophisticated ODE/DAE codes can be applied to the time integration of the PDE.

The MOL has similarities with an approach known as Orthogonal Collocation. The latter approach has been used extensively in environmental engineering to model the unsteady-state in adsorbate concentration that exists in the effluent of a fixed bed of granular activated carbon after introduction of the adsorbate in the feed solution. In this problem, an adsorption front forms and moves through the fixed-bed with time. Its sharpness will depend upon mass transfer properties within the fixed bed. In this approach orthogonal polynomials are used to approximate the solution to the spatial derivatives in the PDEs.

2.3.2 Spatial adaptation

Spatially adaptive methods are methods which can spot regions of high spatial activity, refine the spatial grid in such regions and maintain a sparse grid in regions of low spatial activity. This ensures computationally more efficient simulations by achieving high level of accuracy with relatively low amount of work, [7]. There are two main difficulties in doing this, [6]. The first problem is due to the presence of discontinuities in the solution and their effect on the grid. The second problem is how to organize the algorithm to minimize memory and CPU overhead. Using techniques known as feedback processes, regions requiring refinement (RRR) are located while the solution is in progress using information about the dependent variable obtained at previous time levels [4]. The solution profile at previous time levels is commonly used to estimate the degree of error in a given solution and spatial distribution of the error. The regions requiring refinement are typically those containing the highest degree of solution error.

Sometimes, it is possible to locate the RRR without actually calculating the solution errors by using some error indicators. An error indicator, such as presence of a shock wave or a steep front, will provide enough information to ascertain where to find an RRR. A substantial number of papers on error indicators can be found in the applied mathematics literature [10, 5].

After identifying the regions requiring refinement, we need to devise some strategy to improve the accuracy in the RRR. Three main refinement strategies can be found in the literature, (1) h-refinement (element subdivision), (2) r-refinement (nodal redistribution) and (3) p-refinement (local variation of the order of polynomial approximation).

h-refinement strategy improves the solution accuracy in the RRR by subdividing it into a finer grid [7, 41, 50].

r-refinement methods decrease the spatial step-size by in the RRR by redistributing a fixed number of cells in such a manner that the grid is fine in the RRR and relatively coarse outside RRR [10].

p-refinement methods increase the solution accuracy by increasing the order of the interpolation functions [47].

Combinations of the three refinement procedures are also possible. In particular rh-refinement [39] and hp-refinement [38] methods have gained increasing popularity.

2.3.3 Spatial adaptive solution approach to RE

A few attempts have been made to solve the RE using spatially adaptive methods with both finite difference methods [44] and finite element approaches [1, 18]. The method presented by Ross [44] is an h-method, which he calls *Advancing Front* or the AF Method. This method may be applied to some very special cases only. A very sharp front problem is one of the special cases. The AF method follows a simple algorithm. Given one or more grid points $x_0, x_1, ..., x_n$ at any time, a new point x_{n+1} is added at the next time step. When the lower

boundary is reached the method becomes a fixed grid solution. This point then remains fixed for succeeding steps. Position x_{n+1} is determined along with the values of ψ by solving the volume balance equations. [44] found his method to be 2 to 6 times more efficient than the fixed grid method.

Abriola and Lang [1] present a self-adaptive hierarchic finite element (SHFEM) solution of the one-dimensional RE. This is a p-method in which the local accuracy of the solution is improved by increasing the order of the basis function at the front. This method requires RE to be solved twice at each time step. First, the solution is obtained by solving RE using linear hierarchic basis functions and a fixed grid. Based on this solution, the front is located using the change in effective saturation across the domain. Quadratic basis functions are then added to the equations in the front region. The equation is solved again using the quadratic basis functions, resulting in improved solution quality in the adapted region. Abriola and Lang [1] claim their method to be more accurate and more efficient than the non-adaptive approach, with reduction in CPU time usage by as much as 30%.

Gottardi and Venutelli [18] developed an r type adaption technique based on the moving finite element (MFE) method [23, 2] for a one-dimensional solution of RE. The MFE method is a dynamically adaptive grid finite element method in which grid point locations are made additional dependent variables in a least squares formulation. The solution is expanded in piecewise linear functions, in terms of its value at the grid points and those of the grid point locations on each element, and the square residual so obtained is required to be minimum.

Some Langrangian approaches to solve RE can also be found in the literature. Ewen [15] has proposed a practical moving packet method to solve RE for a vertical flow problem with variably saturated layered porous media.

2.3.4 Adaptive Method of Lines

Most of the ODE solvers automatically adjust the time step-size in order to meet stability and accuracy requirements, still the conventional MOL proceeds in a semi-automatic way since the spatial nodes remain fixed for the entire course of the computation. For problems involving large spatial transitions, such as steep moving fronts or shocks, this conventional method can be inefficient since a large number of uniformly distributed nodes is required to adequately capture the regions of rapidly solution variations. In the regions of low spatial activity, the number of nodes required is much less. Therefore in order to be able to track and resolve important small-scale features with fewest number of nodes, it is necessary to use a procedure that has the ability to add and/or drop nodes as and when required. *Adaptive method of lines* refers to the concept of both *temporal* and *spatial* adaptivity in solving time-dependent PDEs.

Recently, a lot of work has been done on spatially and temporally adaptive MOL. Adaptive MOL has been applied to a variety of problems from different fields of engineering. But, application of spatially adaptive MOL to get a numerical solution of RE has not come to the author's notice. Saucez et al. [45] have applied adaptive MOL to solve the Korteweg-de Vries equation which describes the behavior of small amplitude shallow-water waves in one dimension.

Chapter 3

Approach

3.1 Problem Formulation

RE may be formulated in several ways, [24, 36, 12]. The compressible pressure-head based form of Richards' equation in the vertical direction is used for the present work. The starting point in the derivation of Richards' equation is the mass conservation equation for the aqueous phase in an air-water system where the solid phase is assumed to be immobile, and interphase mass transfer is neglected. Eq. (3.1) is an expression for the conservation mass of the aqueous phase.

$$\frac{\partial(\hat{\rho}(\psi)\theta(\psi))}{\partial t} = -\frac{\partial(\hat{\rho}(\psi)q_z(\psi))}{\partial z} \tag{3.1}$$

and

$$q_z = -K_z(\psi)(\frac{\partial \psi}{\partial z} + \hat{\rho}(\psi)d) \tag{3.2}$$

with

$$K_z = k_r K_s \tag{3.3}$$

$$\rho = \rho_0 e^{\beta(p-p_0)} \tag{3.4}$$

$$\hat{\rho} = \frac{\rho}{\rho_0} \tag{3.5}$$

$$\psi = \frac{p}{\rho_0 ||g||} \tag{3.6}$$

$$d = \frac{g}{||g||} \tag{3.7}$$

$$\tag{3.8}$$

where ρ is the density of the aqueous phase, θ is the volume fraction of the aqueous phase, p is the pressure of the aqueous phase, ρ_0 is the density at p_0, β is the compressibility of the aqueous phase, ψ is the pressure head, K_z is the hydraulic conductivity, k_r is the relative permeability and K_s is saturated conductivity, g is the acceleration due to gravity, z is the vertical spatial dimension, q_z is the Darcy's flow and t is time. The value of d is 1.0 for all the test problems.

On including the Darcy's flow in the mass balance equation we come up with the following equation.

$$\frac{\partial \hat{\rho}(\psi)\theta}{\partial t} = \frac{\partial}{\partial z}[\hat{\rho}(\psi)K_z(\psi)(\frac{\partial \psi}{\partial z} + \hat{\rho}(\psi)d)] \tag{3.9}$$

The pressure head form of RE is derived from the above equation. To obtain the pressure head form of RE we apply the chain rule to the accumulation term. So eq. (3.9) becomes

$$A(\psi)\frac{\partial \psi}{\partial t} = \frac{\partial}{\partial z}[\hat{\rho}(\psi)K_z(\psi)(\frac{\partial \psi}{\partial z} + \hat{\rho}d(\psi))] \tag{3.10}$$

where

$$A(\psi) = \theta\frac{\partial \hat{\rho}(\psi)}{\partial \psi} + \hat{\rho}(\psi)\frac{\partial \theta}{\partial \psi} \tag{3.11}$$

The initial and boundary conditions are

$$\psi(z, t = 0) = \psi_0(z) \tag{3.12}$$

$$\psi(z = 0, t > 0) = \psi_1 \tag{3.13}$$

$$\psi(z = Z, t > 0) = \psi_2 \tag{3.14}$$

where Z = length of the domain, ψ_1 and ψ_2 are pressure heads at the two extremes. ψ_0 can be a function of space.

For a given formulation of RE, an additional set of constitutive relations describing the interdependence among fluid pressures, saturations and relative permeability are required. Over the years, a large number of relationships have been posited [9, 20, 52, 51, 37]. The set of constitutive relations given by van Genuchten [51] and Mualem [37] has been widely used.

$$S_e(\psi) = \frac{\theta_a - \theta_r}{\theta_s - \theta_r} = (1 + |\alpha_v \psi|^{n_v})^{-m_v} \quad for \quad \psi < 0 \tag{3.15}$$
$$S_e(\psi) = 1 \quad for \quad \psi \geq 0$$

where $m_v = 1 - 1/n_v$, S_e is the effective saturation, θ_r is the residual volumetric water content, θ_s is the saturated volumetric water content, α_v is a parameter related to the mean pore-size, and n_v is a parameter related to the uniformity of the pore-size distribution.

It can be seen that S_e is continuously differentiable at $\psi = 0$ if $n_v \leq 1$. If $1 < n_v < 2$, S_e is not continuously differentiable at $\psi = 0$. The specific moisture capacity $c(\psi)$, defined as $d\theta/d\psi$, can be thus calculated using Eq. (3.16) for $\psi < 0$.

$$c(\psi) = \frac{d\theta}{d\psi} = (\theta_s - \theta_r)\frac{dS_e(\psi)}{d\psi} \tag{3.16}$$
$$= (\theta_s - \theta_r) m_v (1 + |\alpha_v \psi|^{-n_v})^{-m_v - 1} n_v \alpha_v |\alpha_v \psi|^{n_v - 1}$$

The relation between saturation and permeability is given by [37]

$$k_r(\psi) = S_e^{1/2}[1 - (1 - S_e^{1/m_v})^{m_v}]^2 \tag{3.17}$$

where k_r is the relative hydraulic conductivity. k_r is an exponentially decreasing function and it takes up values from 0 to 1. It equals almost 1 for saturated soils ($S_e = 1$) and is nearly 0 for small values of S_e. This characteristic relationship between saturation and permeabilty gives rise to sharp fronts of water

moving in the unsaturated zone. Therefore, if there is saturated conditions at the boundary and the soil is dry initially, a quick infiltration and a sharp front is formed.

3.2 Spatial Approximation

We use a relatively straightforward modification of the standard finite difference approach commonly applied to RE [12]. We consider a non-uniform spatial discretization comprised of n_n cells of variable length or cell width Δz_i. Each cell has a node z_i located at its center, except for the ones at the boundary, which have nodes at the extreme cell faces. We will state a definition for the cell width and the internodal distance, which we will follow throughout this work. The cell width $\Delta(z_i)$ is defined as the interval $[z_{i-1/2}, z_{i+1/2}]$, where $z_{i+1/2}$ and $z_{i-1/2}$, are the cell faces. The internodal-distance or $\Delta z_{i+1/2}$ is the distance between nodes z_{i+1} and z_i and is defined as $(\Delta z_{i+1/2} = z_{i+1} - z_i)$ or $(\Delta z_{i+1/2} = 0.5[\Delta(z_i) + \Delta(z_{i+1})])$. The position of each node, except the first one, is calculated as $z_i = z_1 + \sum_{j=1}^{i-1} \Delta(z_j) + 0.5\Delta(z_i)$. The total length of the domain is given by $z_i = \sum_{j=1}^{n_n} \Delta(z_j)$. The spatial operator

$$O_{sdi}(\psi) = \frac{\partial}{\partial z}[\hat{\rho}(\psi)K_z(\psi)(\frac{\partial \psi}{\partial z} + \hat{\rho}(\psi))] \tag{3.18}$$

is approximated at $z = z_i$ for $1 < i < n_n$ by

$$\begin{aligned} O_{sdi}(\psi) &= \Delta z_i^{-1}(\hat{\rho}_{i+1/2}q_{i+1/2} - \hat{\rho}_{i-1/2}q_{i-1/2}) \\ q_{i+1/2} &= -K_{i+1/2}(\frac{\Delta\psi_{i+1/2}}{\Delta z_{i+1/2}} + \hat{\rho}_{i+1/2}) \end{aligned} \tag{3.19}$$

where n_n is the number of unknowns in the solution, q is the Darcy's velocity and ψ_i is the approximation to $\psi(z_i)$.

$$K_{z,i+1/2} = \frac{\Delta z_i K_{z,i+1} + \Delta z_{i+1} K_{z,i}}{2\Delta z_{i+1/2}} \tag{3.20}$$

$K_{z,i+1/2}$ and $K_{z,i-1/2}$ are the values of hydraulic conductivity calculated, at the respective cell faces, as a weighted mean of their values at the respective nodes.

The DAE system that we solve is a system of n_n differential equations for the n_n unknown functions of t and $\psi_i(t)$, subject to first kind boundary conditions ψ_1 and ψ_{n_n}. The ith equation is

$$A(\psi_i)\frac{d\psi_i}{dt} = O_{sdi}(\psi) \tag{3.21}$$

where $A(\psi_i)$ is obtained from eq. (3.11)

3.3 Time Integration

3.3.1 Introduction

As mentioned earlier, the present work is essentially an extension of [30], with spatial adaptation added to enhance the numerical accuracy and efficiency of the method. Significant details of the time integration and temporal adaptation are available in the literature [8, 30, 29]. We provide a summary of the time discretization to make clear what is required to incorporate the adaptive spatial discretization into the DAE/MOL approach. The most common approach, the BDF approach, has been used for solving DAEs. The complete details of this approach are covered in [8].

DAEs of general non-linear, fully implicit vector form

$$F(t, y, y') = 0 \tag{3.22}$$

have been used, where $t \in \Re, y, y' \in \Re^n$, and $F : \Re^{2n+1} \rightarrow \Re^n$. The function F is called the residual function. Equations in the system described by [8] are

some combination of ODEs and algebraic equations. An initial value problem (IVP) consists of a DAE and a set of initial values t_0, y_0, y'_0. For a given IVP, the methods presented in this work generate a numerical approximation to the solution at a finite number of times on an interval $[t_0, T]$.

3.3.2 Time integration algorithm

The following are the steps involved in solving DAEs based on a BDF approach.

1. The solution of the DAE is predicted by extrapolating from previously computed points in the solution history with a Lagrange polynomial of a suitable order.

2. A corrector equation is formed for the unknown solution vector y_{n+1} using a Lagrange polynomial of suitable order that terminates at the unknown solution point.

3. The nonlinear corrector equation is solved to an appropriate error tolerance if possible, or else the step-size and/or order is reduced and solved again.

4. The solution history is updated.

5. Allowable step-size and order of the solution is approximated for the next step.

6. If the solution information is desired, it is output after any required interpolation.

Generally, in BDF methods the derivative of a Lagrange polynomial is substituted for the derivative appearing in the DAE to produce a nonlinear system. The solution of the nonlinear algebraic system approximates the solution of the DAE. The Lagrange polynomial passes through the unknown solution at the current time and interpolates a finite number of previously approximated solution

points (the solution history). To develop these ideas further, we consider briefly the fixed leading coefficient BDF FLCBDF predictor/corrector formulation implemented in this work. Given $k+1$ previous solutions for y, a Lagrange predictor polynomial is constructed through the solution such that

$$\omega^p_{k,n+1}(t_{n-i}) = y_{n-i}, \qquad i = 0, 1, ..., k \tag{3.23}$$

where ω is a Lagrange polynomial expression, p indicates that it is a predictor expression, k denotes the order, which ranges between a value of 1 and 5 and $n+1$ is a time step index that refers to the time for which the solution is sought. This polynomial gives an explicit approximation for the solution and it's derivative at t_{n+1}, given by

$$y^p_{n+1} = \omega^p_{n+1}(t_{n+1}) \tag{3.24}$$

$$y'^p_{n+1} = \omega'^p_{n+1}(t_{n+1}) \tag{3.25}$$

A Lagrange corrector polynomial of kth order is then constructed and its value is implicitly defined at t_{n+1} by requiring that it satisfies the DAE at t_{n+1}. Hence, the corrector polynomial satisfies the conditions:

$$\omega^c_{k,n+1}(t_{n-i} - ih_{n+1}) = \omega^p_{k,n+1}(t_{n-i} - ih_{n+1}) \qquad i = 1, ..., k \tag{3.26}$$

$$F(t_{n+1}, \omega^c_{k,n+1}(t_{n+1}), \omega'^c_{k,n+1}(t_{n+1})) = 0 \tag{3.27}$$

where $\omega^c_{k,n+1}(t_{n+1}) = y'^c_{n+1}$ is the FLCBDF for the derivative at t_{n+1} and h_{n+1} is the temporal step-size taken to solve for y_{n+1}.

It has been shown in [26] that

$$\omega^p_{n+1}(t_{n+1}) = y'^p_{n+1} + \alpha(y^c_{n+1} - y^p_{n+1}) \tag{3.28}$$

where

$$\alpha = \frac{\alpha_0}{h_{n+1}} = \frac{1}{h_{n+1}} \sum_{j=1}^{k} 1/j \tag{3.29}$$

The key feature of this approach is that α remains fixed unless the order or step-size changes.

3.3.3 Solution of algebraic systems

The solution at a required time t_{n+1} is obtained by solving a system of algebraic equations for y^c_{n+1}. The system of equations in terms of the predictor-corrector scheme is

$$F[t_{n+1}, y^c_{n+1}, y'^p_{n+1} + \alpha(y^c_{n+1} - y^p_{n+1})] = 0 \tag{3.30}$$

The above equation in simplified notation is

$$F(t, y, \alpha y + \beta^n) = 0 \tag{3.31}$$

where all the variables are evaluated at t_{n+1} and $\beta^n = (y'^p_{n+1} - \alpha y^p_{n+1})$.

For RE, the system of DAEs is nonlinear in y and y', therefore eqn. (3.31) is a nonlinear system of algebraic equations. A modified Newton iteration method or chord method,, [32] is used to solve the system of nonlinear equations. In the chord method the Jacobian is not updated after each iteration, but is reused for multiple iterations and over multiple time steps. The Jacobian is updated when the solution order or the time step have changed so much that the modified Newton iteration converges slowly or fails to converge.This approached is based on the assumption that the solution from the previous time step is often a good predictor of the solution for the following time step (this happens when the time variation is smooth). Under these type of conditions, three or fewer nonlinear iterations are typically required.

3.4 Spatial Adaptive Approach

3.4.1 h-adaptation

In h-adaptation, the grid is refined by adding new cells to the regions where sharp fronts are developed. The main advantage of h-adaptation is the ability to keep the elements from being overly distorted. The principal disadvantage

associated with this method is that the size of the grid changes due to addition or removal of nodes.

3.4.2 Algorithm

The solution process using h-type spatial adaptation can be described in the following steps:

1. Construct the initial grid and set the initial and boundary conditions.
2. Solve the system for ψ, for $[t, t + \Delta t]$, starting initially with $t = 0$.
3. Compute the error indicator in each cell. Determine if adaptation is necessary.
4. Proceed normally if adaptation is not required. If adaptation is required at $t + \Delta t$, adapt the grid and interpolate the ψ values and the solution history for the new grid and proceed.
5. Continue till the time at which solution output is required is reached.

3.4.3 Selection of error indicator

Change in saturation per unit length is chosen as the error indicator to tell where adaptation is required, [1]. The following condition on the saturation is used as an error indicator:

$$\frac{|S_e(i+1) - S_e(i)|}{\Delta z_{i+1/2}} \geq \sigma \quad 1 = 1, 2, ..., n_n \tag{3.32}$$

The saturation serves as a non-linear normalization of the pressure head, and ranges from a value of 0 to 1.0. Therefore σ is a criterion based upon the maximum permissible gradient of a non-linearly normalized variable.

3.4.4 Grid adaptation procedure

We now describe in detail the, actual implementation of h-refinement to achieve spatial adaptation in the MOL solution of RE. The physical domain is divided into N_{base} number of coarse cells, which we term as the base-cells. These base-cells remain fixed throughout the simulation. Once we determine the location of the front on the physical domain, we find the corresponding base-cell in which it lies and that base-cell is then discretized into finer sub-cells. At a particular time, the front is located using the error indicator. If error in any cell exceeds a prescribed tolerance value, that particular cell is marked as a cell requiring refinement. The size of the resulting cells depend on the value of the maximum error in that base-cell. It is possible that a base-cell which was finely discretized initially can be coarsened into a smaller number of cells depending on the maximum error value in that base cell. Multiple levels of discritization are also possible, i.e. we can have different levels of discretization for different base-cells depending on the maximum value of the error in that base-cell.

Adapting the grid at each time step has some computational costs associated with it; so it may not be advisable to carry out adaptation after every time step. Thus, adaptation is carried out at each Δt_{adapt}. $\Delta t_{adapt}$is provided by the user. The criterion and guidance for the choice of Δt_{adapt} is discussed later. It is required that a fine grid be maintained in the region where the front will move in the time interval $[t, t + \Delta t_{adapt}]$. To predict the position of the front we need to know how fast it is moving and in which direction. We estimate the velocity (v) using the following formula:

$$v = \frac{dz}{dt} = \frac{d\psi}{dt} / \frac{d\psi}{dz} \tag{3.33}$$

or in discretized form the velocity at the ith node is

$$v_i = \frac{d\psi_i}{dt} / (\frac{\psi_{i+1} - \psi_i}{\Delta z_{i+1/2}}) \tag{3.34}$$

Since the value of $d\psi/dt$ is available to us at each time step, the velocity can be

calculated cheaply. Once we obtain the velocity, we calculate the distance it will travel in Δt_{adapt} ($=v\Delta t_{adapt}$). This entire region is then refined.

For purpose of comparison of the non-uniform adaptive grid with a uniform grid we define a term *Level of Adaptation* or LoA, which is a measure of the finest discretization maintained at the front region. For example, an irregular grid with LoA=401 that Δz maintained at the front region equals Δz of an uniform grid with 401 nodes. Thus, for uniform discretization the LoA is same as the number of nodes.

3.4.5 Interpolation of ψ-values on the adapted grid

Once the grid is adapted, the ψ values on the initial grid need to be interpolated for the new grid before the simulation can resume. Since, in the FLCBDF approach, a Lagrange polynomial is used to interpolate the solution history to find an explicit approximate value for the solution and its derivative, we also need to adapt the solution history for the new grid. The actual interpolation can be achieved using any number of the popular methods, like linear interpolation, Lagrangian interpolation, Hermite interpolation or a cubic spline. We used a simple linear interpolation in this work.

Mass conservation is a fundamental property of the physical solution that should be maintained by the numerical solution. Special care is required to maintain mass balance in the adaption process. To make sure that mass is conserved, total mass in each base-cell should be equal before and after adaptation. This is ensured by using the following approach: if in a particular base-cell i there are n number of sub-cells, then the total moisture content in that base-cell is given by

$$\textit{total moisture content} = \sum_{j=1}^{n} \tilde{\rho}_{i,j}\theta_{i,j}\Delta z_{i,j} \tag{3.35}$$

To make sure that mass is conserved in that particular cell in the process of adaptation, the total moisture content before and after adaptation is maintained

to be the same, as the base cells are fixed throughout our simulation.

3.5 Implementation Details

The DAE/MOL code was the one developed in [30] (which is a mixed language environment) and the spatial adaption was implemented in C++. All the numerical simulations were done on dedicated machines running RedHat Linux 7.1 with 500 MHz processors, 512 kilobytes of cache, and 768 megabytes of RAM. The codes were compiled with g++/gcc/g77 version 2.96.

Chapter 4

Results and Discussion

4.1 Introduction

Before stating the numerical results needed to satisfy the objectives of this work, we describe the three test problems on which these investigations are based and discuss the methods for estimating the accuracy and efficiency of the given method. The main aim of the numerical experiments performed was to (1) to validate the spatially adaptive MOL method for RE by comparison to results from a standard, uniform grid solution for a series of test problems, (2) to evaluate the relative efficiency of the spatially adaptive approach, and (3) to investigate the methods of improving the efficiency of the solutions.

4.2 Test Problems

The space-time adaptive MOL method was applied to three sets of test conditions: (1) Simple vertical infiltration (SVI), (2) Vertical infiltration with redistribution (VIR), and (3) Constant Recharge (CR). The simulation conditions have been tabulated in table 4.1, including constitutive relation properties, spatial and temporal domains and auxiliary conditions. The material properties for all three problems correspond to a dune sand as reported by [34]. The simula-

tion conditions for all the test problems yield a difficult sharp-front problem. All three problems have drained-to-equilibrium initial conditions.

Table 4.1: Simulation Conditions

Variable	SVI problem	VIR problem	CR problem
θ_r (-)	9.3e-2	9.3e-2	9.3e-2
θ_s (-)	3.01e-1	3.01e-1	3.01e-1
$\alpha_v(m^{-1})$	5.47	5.47	5.47
n_v	4.264	4.264	4.264
$K_s(m/day)$	5.04	5.04	5.04
$S_s(m^{-1})$	1.0e-6	1.0e-6	1.0e-6
$\Omega(m)$	[0,10]	[5, 10]	[0, 10]
$t(days)$	[0,0.3]	[0, 0.5]	[0, 0.3]
$\psi_0(m)$	-z	-z	-z
$\psi_1(m)$	0.1	$-10(1.0 - 1.0e^{-t})$	-
$\psi_2(m)$	0.0	0.0	0.0
$q^{z=0}_{w,n_n-1}(m/day)$	-	-	5

The SVI problem is a common test problem [48, 35]. It represents a problem with constant head boundary conditions both at the top and the bottom and drained-to-equilibrium initial condition. This situation can arise when there is a water table at the bottom boundary and a source of water, with a constant pressure head, is developed at the top boundary. The VIR problem also has drained-to-equilibrium initial conditions but in this case the pressure head maintained at the top boundary is not constant but is a function of time. This might correspond to an initial precipitation causing a source of water at the top boundary but this source gradually diminishes with time causing the pressure head to fall exponentially with time. This causes development of a sharp front which gradually tails off with time. The CR problem is a simple test problem

to analyse the mass-conservation properties of our method. This corresponds to a simple case of presence of a water table at the bottom boundary and a source causing a constant recharge at the top boundary. The above three set of test conditions represent a majority of physical situations that may arise in the real world.

4.3 Error and Work Measures

We will now briefly define the work and error measures used in this work to analyze the numerical solutions obtained by the various simulations. We will outline two measures of error and one measure of work.

Mass balance error is a traditional error measure for RE. We consider the discrete mass balance error as used by [31]. The mass balance error is calculated using the following equation

$$\epsilon_m = |1 - \frac{\sum_{i=0}^{n_n} [\rho_i \theta_i(t) - \rho_i \theta_i(0)] \Delta x}{-\int_0^t [q^{bc}(L) + q^{bc}(0)] dt}| \tag{4.1}$$

where $q^{bc}(L)$ and $q^{bc}(0)$ are the outward normal mass fluxes at the boundaries.

We also use the difference of the highly resolved uniform-grid solution and the obtained solution as a measure of error.

$$\epsilon = \left\{ \epsilon_i = \psi_i - \hat{\psi}_i | i = 0, ..., n_n - 1 \right\} \tag{4.2}$$

. where $\hat{\psi}_i$ is the point on the dense grid corresponding to the coarse grid location. The dense-grid solutions for the SVI problem and the VIR problem, were both obtained on a uniform grid of 3201 nodes, with the absolute tolerance (ϵ_a) and the relative tolerance (ϵ_r) both set to 1.0e-6. L_1 norm of the error was used as a measure of total error.

$$\epsilon_{L_1} = \frac{\sum_{i=1}^{n_n} |\epsilon_i| \Delta z_i}{\sum_{i=1}^{n_n} \Delta z_i} \tag{4.3}$$

The main objective when measuring work is to compare the performance of the spatially and temporally adaptive method with that of a temporally adaptive code with uniform and fixed grid. We also study the characteristics of the codes relative to changes in the level of adaptation and the number of cells in the base grid. Thus, CPU time was considered as suitable choice for measure of work.

4.4 Numerical Comparisons

Each test case was run with ϵ_a and ϵ_r both set to 1.0e-6. The SVI and the VIR problems were run for five LoA values, $n_n = 51, 101, 201, 401, 801$ and various number of cells in the base grid.

Figure 4.1 and figure 4.2 are uniform grid and adaptive grid solutions of the SVI problem for time step-size of 0.025 days. The first subplot shows the pressure head profile on the y-axis against the depth on the x-axis. The second subplot shows the discretization pattern corresponding to each time step. The simulations were run till a time of 0.3 days was reached. Each of the vertical line in the above mentioned figures correspond to the sharp front at that particular time and we can clearly see the sharp front moving towards the left starting from $z = 10m$. For the uniform grid solution $N = 401$ as compared to only 133 nodes required by the adaptive grid approach. It should be noted that the level of refinement at the front location is same for both the solutions. Δt_{adapt} for the adaptive solution was 0.025 days. A comparison of some of the computational statistics (i.e. the number of nodes N, the number function evaluations FUNC, the number of Jacobian evaluations JACS, the number of steps taken STEPS, and the total computational time taken TIME) from the various runs for the two approaches have been tabulated in table 4.2. Figure 4.3 is a plot of moisture content profile obtained from the adaptive approach. Figures 4.4 and 4.5 show a plot of L_1 norm of the total error versus total number of nodes used and the

total time taken respectively.

It should be observed from the above figures that the fronts are so sharp that, even for 401 nodes, there are less than three nodes defining the steep front. The maximum errors are concentrated at the front and these dominate the overall error. L_2 and L_{Inf} norms of the error magnify these errors. Therefore, the choice of L_1 norm for the measure of total error has been made. The errors for the same LoA for the adaptive and the non-adaptive case are comparable, although there are considerably less number of equations to be solved for the adaptive case and thus the CPU time requirement is about 2.5-3 times less. Also, for the same amount of computational effort, the level of accuracy achieved by the adaptive method is much higher than the non-adaptive method. The gain in CPU time is more marked as we increase the LoA, this can be explained by the fact that for a higher value of LoA.

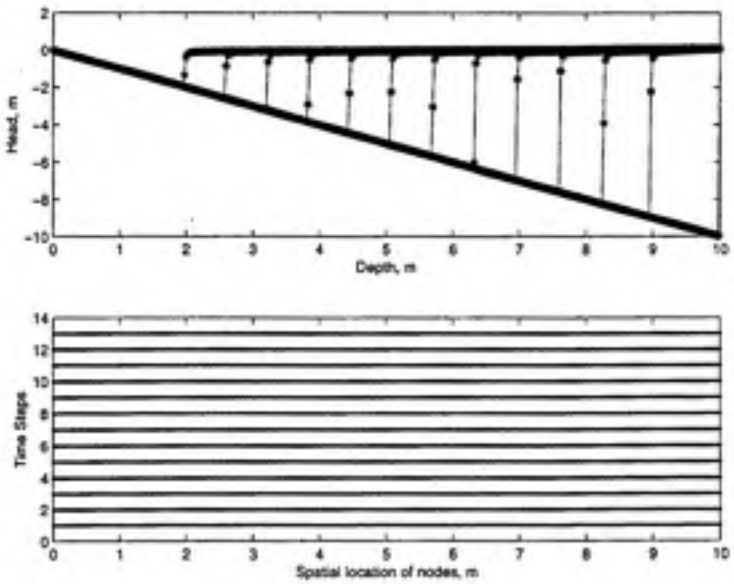

Figure 4.1: SVI problem - pressure head profile (uniform grid, LoA=401 nodes).

Solution profile for the VIR problem using the adaptive MOL approach and the uniform grid approach can be seen in figures 4.6 and 4.7 respectively. These

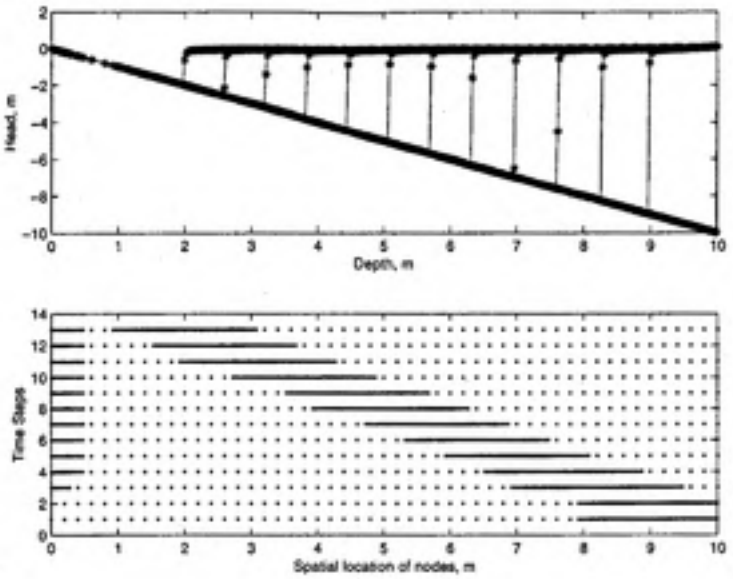

Figure 4.2: SVI problem - pressure head profile (adaptive grid, LoA=401 nodes).

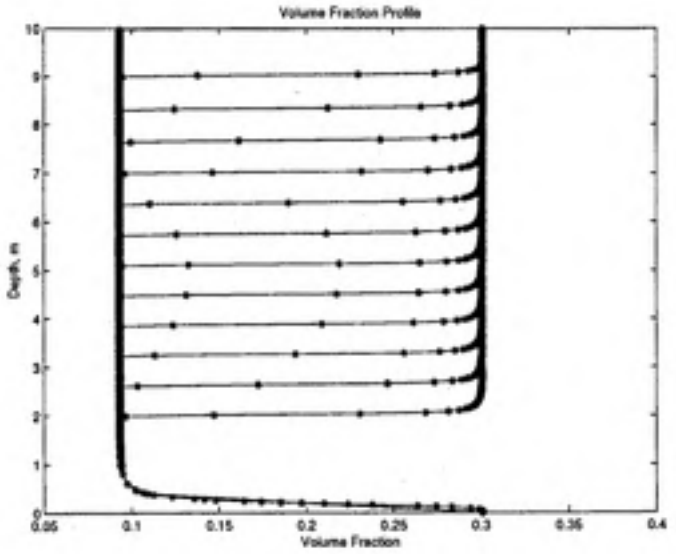

Figure 4.3: SVI problem - moisture content profile (adaptive grid, LoA=401 nodes).

results correspond to 801 nodes for the uniform grid and the time step-size is is 0.0625 days and the simulation was run till $t = 0.5$ days. The value of Δt_{adapt}

Table 4.2: Computational Statistics and L_1-Norm of the Error for SVI problem

Grid	N	LoA	FUNC	JACS	STEPS	TIME	ϵ_{L_1}
Uniform	51	51	16517	4638	4167	17	4.032e-02
Uniform	101	101	14977	4670	4386	30	1.471e-02
Uniform	201	201	26951	8228	7726	104	8.489e-03
Uniform	401	401	50871	15172	14186	387	4.353e-03
Uniform	801	801	96228	28066	26128	1465	2.734e-03
Adaptive	51	51	16517	4638	4167	17	4.034e-02
Adaptive	62	101	17882	4987	4700	22	1.504e-02
Adaptive	85	201	29437	8941	8424	52	7.622e-03
Adaptive	133	401	54213	16653	15697	147	4.295e-03
Adaptive	227	801	102327	31000	29115	466	2.690e-03

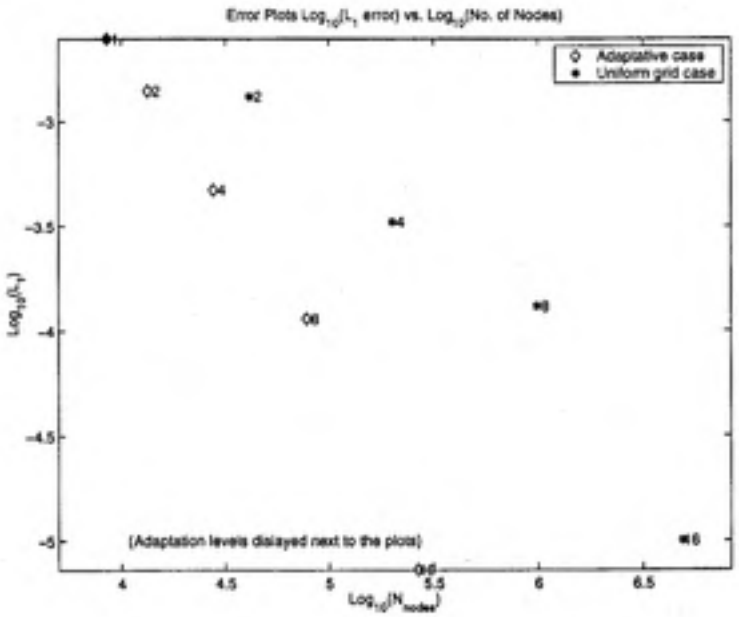

Figure 4.4: Total nodes-error plot for SVI problem.

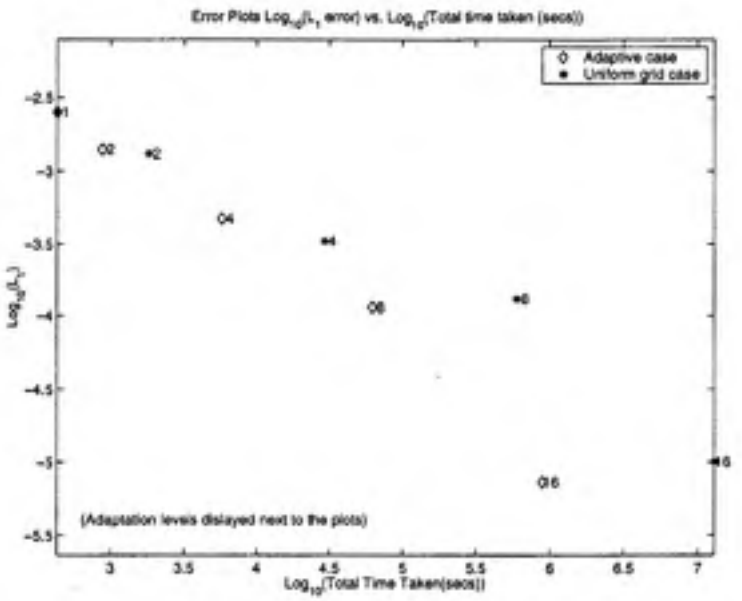

Figure 4.5: CPU time-error scatter plot for SVI problem.

was 0.0125 days. Figure 4.3 is a plot of volumetric water content after every time interval of 0.0625 days. It is evident from the figure, for the VIR problem, that there is a rapid infiltration of water from the surface, followed by a period of redistribution of the water due to the episodic nature of the recharge from the top boundary. Figure 4.9 shows the pressure head profile w.r.t. time at the top boundary. Figures 4.10 and 4.11 show a plot of L_1 norm of the total error versus total number of nodes used and the total time taken respectively. Table 4.3 contains the computational statistics and error calculations for the solution of the VIR problem. From the table it can be seen that the adaptive MOL is 2 to 3 times faster than the standard MOL.

The main motivation for solving the CR problem was to test the mass-conservation properties of the adaptive MOL method. This problem is similar to the SVI problem, excepting the top boundary condition. In the CR problem the top boundary condition is Neumann type, with a constant flux of water ($q_w^{z=0}$), as compared to the Dirichlet type constant head boundary condition of the SVI

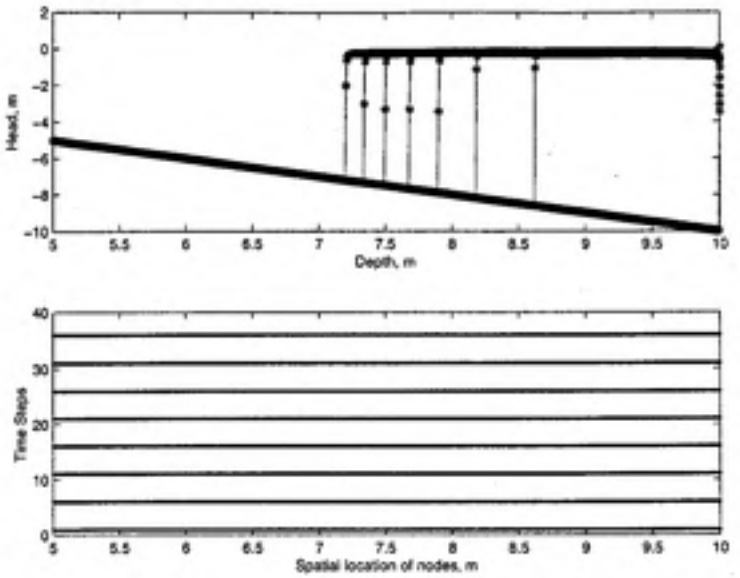

Figure 4.6: VIR problem - pressure head profile (uniform grid, LoA=801 nodes).

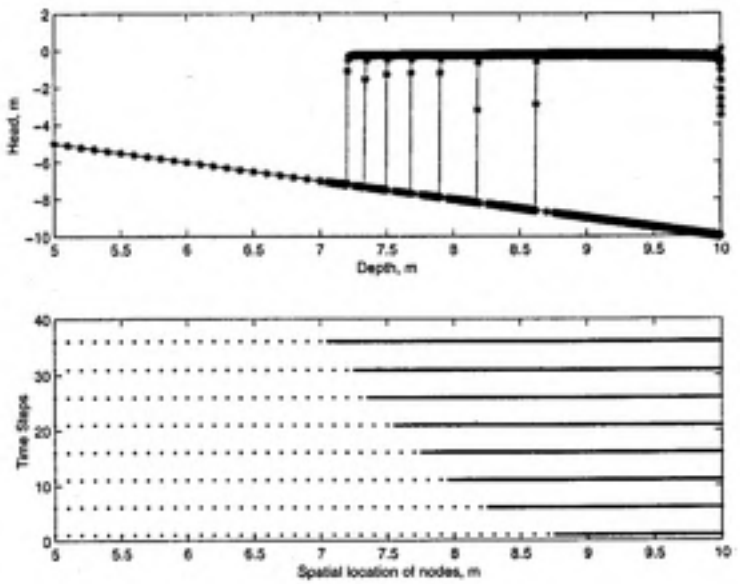

Figure 4.7: VIR problem - pressure head profile (adaptive grid, LoA=801 nodes).

problem. A constant head boundary condition induces a time dependent flow boundary condition. The motivation behind using a constant flux at the bound-

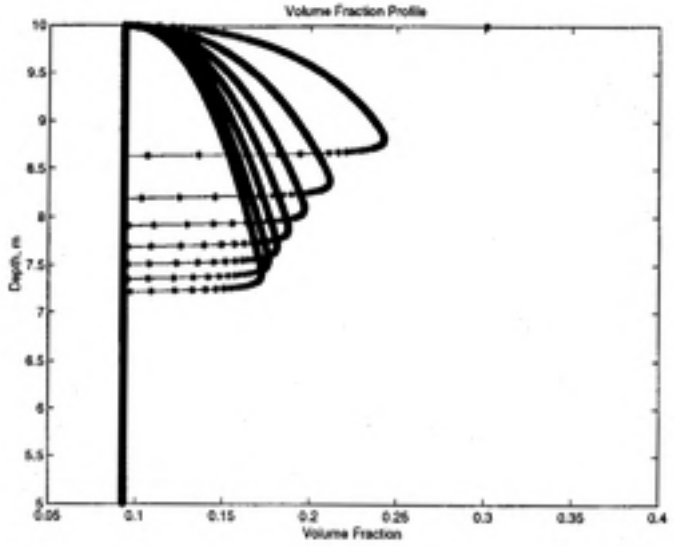

Figure 4.8: VIR problem - moisture content profile (adaptive grid, LoA=801 nodes).

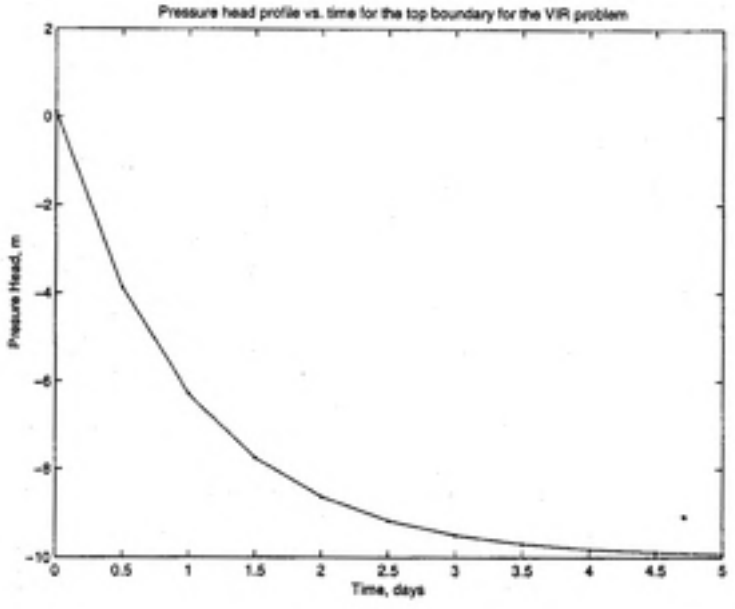

Figure 4.9: Pressure head profile vs. time for the top boundary for the VIR problem.

ary is that it makes easy the mass balance calculations because at any time t the amount of water entering the system is simply given by $q_w^{z=0}t$, with a front

Table 4.3: Computational Statistics and L_1-Norm of the Error for VIR problem

Grid	N	LoA	FUNC	JACS	STEPS	TIME	ϵ_{L_1}
Uniform	51	51	7057	2268	2123	8	1.511e-01
Uniform	101	101	12485	3984	3727	27	6.629e-02
Uniform	201	201	22366	7000	6502	92	7.734e-02
Uniform	401	401	42168	12859	11935	343	2.684e-02
Uniform	801	801	79154	23449	21635	1300	1.597e-02
Adaptive	51	51	7057	2268	2123	8	1.511e-01
Adaptive	69	101	13581	4312	4086	21	8.321e-02
Adaptive	101	201	23951	7606	7155	56	7.223e-02
Adaptive	168	401	43405	13516	12591	167	2.958e-02
Adaptive	296	801	81802	24841	23134	555	1.295e-02

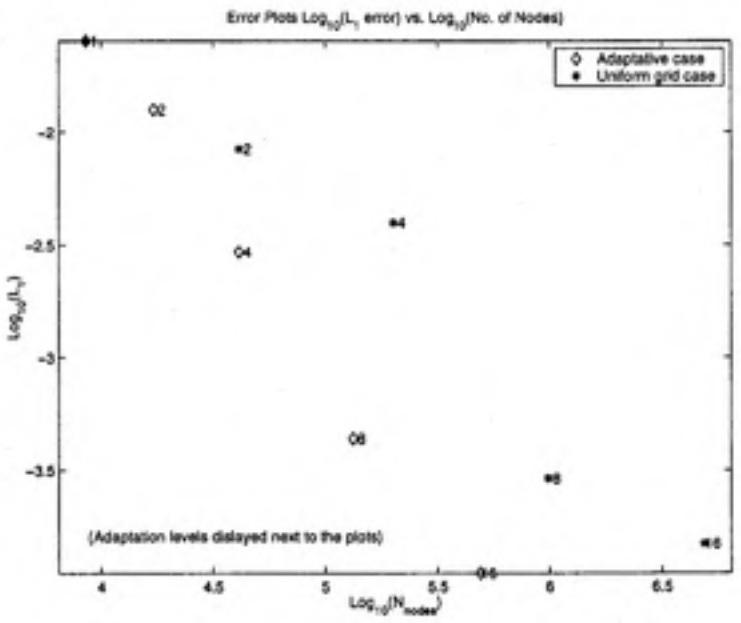

Figure 4.10: Total nodes-error scatter plot for VIR problem.

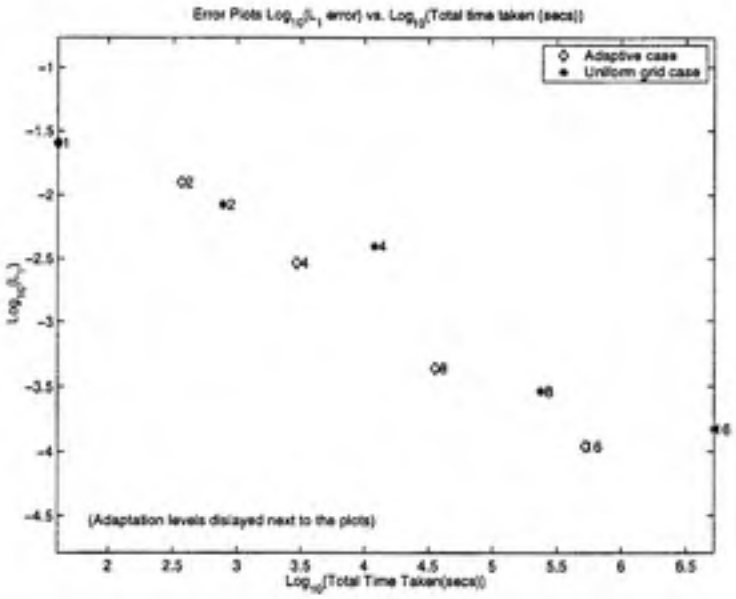

Figure 4.11: CPU time-error scatter plot for VIR problem.

similar to the constant head boundary condition being developed. Figures 4.12 and 4.13 show the uniform-grid and adaptive grid solution of the CR problem and figure 4.14 shows the volumetric moisture content profile. The mass balance errors for different runs of the adaptive method and their comparison with the fixed grid method has been tabulated in the table 4.4. The mass balance errors for the standard MOL and adaptive MOL are nearly the same, thus we can safely say that the mass conservative properties of the FLCBDF method is not lost by the process of spatial adaptation.

On close observation of the above tables of computational statistics for all the three test problems, one can clearly see that, for the same LoA, the FUNC, JACS and STEPS are nearly the same for the adaptive and non-adaptive MOLs, although there are considerable fewer number of equations to be solved for the former and the CPU time requirement is much less for the same. This can be explained by the fact that the statistics like FUNC, JACS and STEPS depend on the equations to be solved at the front region and the spatial discretization at

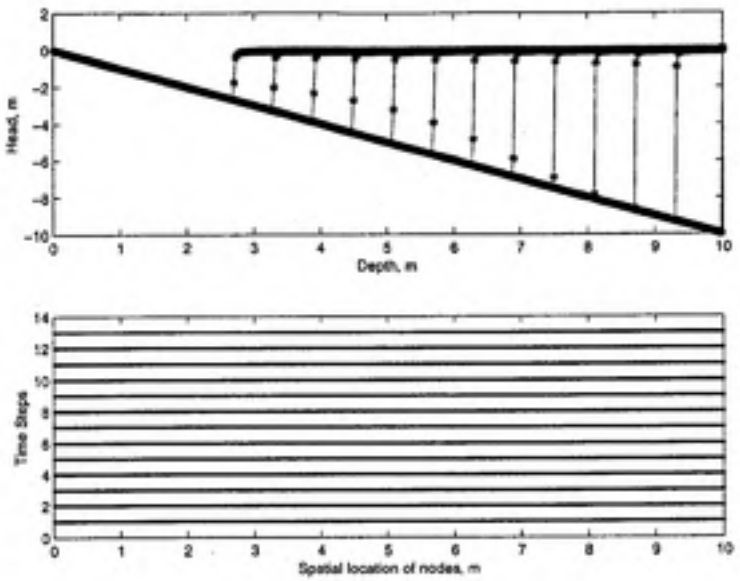

Figure 4.12: CR problem - pressure head profile (uniform grid, LoA=401 nodes).

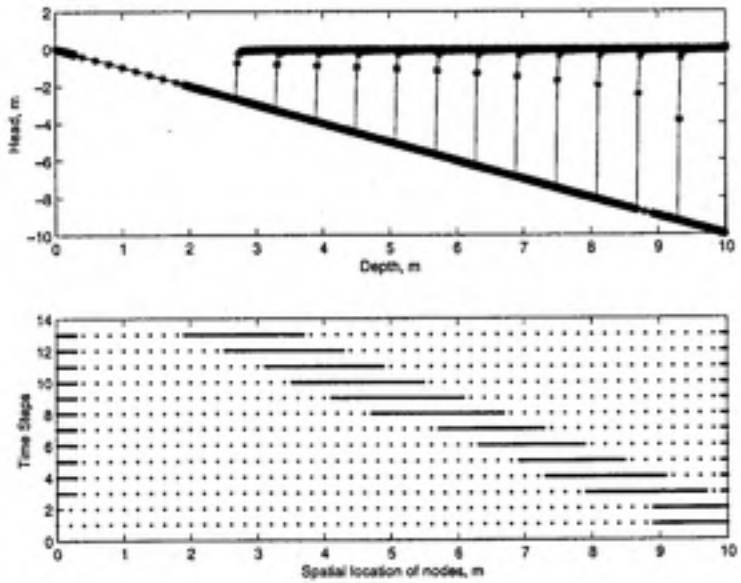

Figure 4.13: CR problem - pressure head profile (adaptive grid, LoA=401 nodes).

the front. Since the base-cells are fixed throughout the simulation, the physical location of the nodes (and thus the Δz) at the front are identical for both the

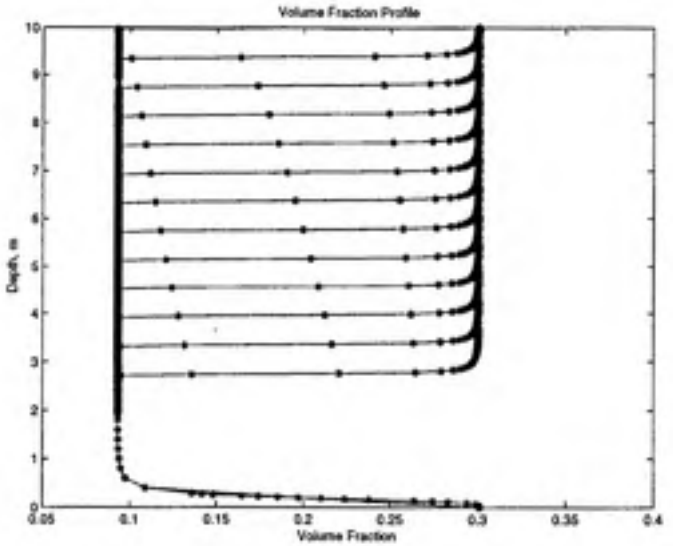

Figure 4.14: CR problem - moisture content profile (adaptive grid, LoA=401 nodes).

Table 4.4: Computational Statistics and Mass Balance Error for the CR Problem

Grid	N	LoA	FUNC	JACS	STEPS	TIME	ϵ_m
Adaptive	81	201	27641	8369	7906	147	6.538e-04
Adaptive	119	401	50860	15584	14721	405	6.528e-04
Uniform	201	201	24999	7686	7234	327	1.262e-4
Uniform	401	401	47386	14180	13277	1217	1.264e-04

methods, but since there are a lesser number of equations to be solved, the CPU time requirement is much less.

The choice of Δt_{adapt} and the number of base-cells are also crucial to the performance of the adaptive method. If we choose a very small Δt_{adapt}, the RRR $(= v\Delta t_{adapt})$ will be small with fewer unknowns, fewer equations to be solved, and thus lower CPU time requirement. But this also means more frequent adaptation of the grid with added computational expense. Knowing that their is some loss

of computational time associated with every adaptation process, we need to choose an optimal value of Δt_{adapt} balancing the expense associated incurred by regridding with the desire to limit the size of the RRR. Also, the choice of number of base-cells needs to be made carefully. We do not want to have a large number of base-cells because we would be wasting some nodes in the regions where a dense grid is not required. On the other hand, a small number of base-cells can lead to inaccurate results in the coarse regions.

Chapter 5

Conclusions

In this work we formulate a variable space-time discretization for a finite difference solution of RE and outlined a method of h-type spatial adaptation implemented in the MOL frame. We can now draw the following conclusions based on our analysis:

1. h-type spatial adaptation can be successfully implemented in the DAE/MOL framework to obtain efficient and robust finite difference solution of RE.

2. Same level of accuracy as a uniform grid solution can be achieved by using adaptive MOL and having to solve a lesser number of nodes and with considerable savings in computational effort and time.

3. The mass conservation properties of the adaptive MOL approach to solve RE are comparable to the standard uniform grid MOL approach.

4. The performance of the adaptive approach depends on the number of base-cells used and the choice of Δt_{adapt}. The advantage of the adaptive approach is more conspicuous as more accurate solution is required, and the level of adaptation is increased.

REFERENCES

[1] L. M. Abriola and J. R. Lang. Self-adaptive hierarchic finite element solution of the one-dimensional unsaturated flow equation. *International Journal for Numerical Methods in Fluids*, 10:227–246, 1990.

[2] T. Arbogast, M. F. Wheeler, and N. Y. Zhang. A nonlinear mixed finite element method for a degenerate parabolic equation arising in flow in porous media. *SIAM Journal on Numerical Analysis*, 33(4):1669–1687, 1996.

[3] C. Babajimopoulos. A douglas-jones predictor-corrector program for simulating one-dimensional unsaturated flow in soil. *Soil Science*, 29(2):267–270, 1991.

[4] I. Babuška and W. Gui. Basic principals of feedback and adaptive approaches in the finite element method. *Computer Methods in Applied Mechanics and Engineering*, 55:27–42, 1986.

[5] R. E. Bank and R. K. Smith. Mesh smoothing using a posteriori error estimate. *SIAM Journal on Numerical Analysis*, 34(3):979–997, 1997.

[6] M. J. Berger and A. P. Collela. Local adaptive mesh refinement for shock hydrodynamics. *Journal of Computaional Physics*, 82(1):64–84, 1989.

[7] M. J. Berger and J. Oliger. Adaptive mesh refinememt for hyperbolic partial-differential equations. *Journal of Computaional Physics*, 53(3):484–512, 1984.

[8] K. E. Brenan, S. L. Campbell, and L. R. Petzold. *The Numerical Solution of Initial Value Problems in Differential-Algebraic Equations.* Society for Industrial and Applied Mathematics, Philadelphia, PA, 1996.

[9] R. H. Brooks and A. T. Corey. Hydraulic properties of porous media. Technical Report paper number 3, Colorado State University, Fort Collins, CO, 1964.

[10] W. M. Cao, W. Z. Huang, and R. D. Russell. Comparison of two-dimensional r-adaptive finite element methods using various error indicators. *Mathematics and Computers in Simulation*, 56(2):127–143, 2001.

[11] M. A. Celia and P. Binning. A mass conservative numerical solution for two-phase flow in porous media with application to unsaturated flow. *Water Resources Research*, 28(10):2819–2828, 1992.

[12] M. A. Celia, E. T. Bouloutas, and R. L. Zarba. A general mass-conservative numerical solution for the unsaturated flow equation. *Water Resources Research*, 26(7):1483–1496, 1990.

[13] J. C. Critteden, B.W. C. Wong, W. E. Thacker, V. L. Snoeyink, and R. L. Hinrichs. Mathematical model of sequential loading in fixed-bed adsorbers. *Journal Water Pollution Control Federation*, 52(11):2780–2795, 1980.

[14] A. I. Elkadi and G. Ling. The courant and peclet number criteria for the numerical solution of the richards equation. *Water Resources Research*, 29 (10):3485–3494, 1993.

[15] J. Ewen. Moving packet model for variably saturated flow. *Water Resources Research*, 36(9):2587–2594, 2000.

[16] P. A. Forsyth, Y. S. Wu, and K. Pruess. Robust numerical methods for saturated-unsaturated flow with dry initial conditions in heterogeneous media. *Advances in Water Resources*, 18:25–38, 1995.

[17] R. A. Freeze. Three-dimensional, transient, saturated-unsaturated flow in a groundwater basin. *Water Resources Research*, 7(2):347–366, 1971.

[18] G. Gottardi and M. Venutelli. Moving finite-element model for one-dimensional infiltration in unsaturated soil. *Water Resources Research*, 28 (12):3259–3267, 1992.

[19] G. Gottardi and M. Venutelli. One-dimensional moving finite-element model of solute transport. *Ground Water*, 32(4):645–649, 1994.

[20] R. Haverkamp, J. Vauclin, J. Touma, P. J. Wierenga, and G. Vachaud. A comparison of numerical simulation models for one-dimensional infiltration. *Soil Science Society of America Journal*, 41:285–294, 1977.

[21] D. Hillel. *Fundamentals of Soil Physics.* Academic Press, New York, NY, 1980.

[22] R. G. Hills, I. Porro, D. B. Hudson, and P. J. Wierenga. Modeling one-dimensional infiltration into very dry soils, 1. model development and evaluation. *Water Resources Research*, 25(6):1259–1269, 1989.

[23] R. Huber and R. Helmig. Multiphase flow in heterogeneous porous media: A classical finite element method versus an implicit pressure-explicit saturation-based mixed finite element-finite volume approach. *International Journal for Numerical Methods in Fluids*, 29:899–920, 1999.

[24] P. S. Huyakorn and G. F. Pinder. *Computational Methods in Subsurface Flow.* Academic Press, Orlando, FL, 1983.

[25] P. S. Huyakorn, S. D. Thomas, and B. M. Thompson. Techniques for making finite elements competitive in modeling flow in variably saturated porous media. *Water Resources Research*, 20(8):1099–1115, 1984.

[26] K. R. Jackson and R. Sacks-Davis. An alternative implementation of variable step-size multistep formulas for stiff ODEs. *ACM Transactions in Mathematical Software*, 6:295–318, 1980.

[27] S.-H. Ju and K.-J. S. Kung. Mass types, element orders and solution schemes for the Richards equation. *Computers and Geosciences*, 23(2):175–187, 1997.

[28] Z. J. Kabala and P. C. D. Milly. Sensitivity analysis of flow in unsaturated heterogeneous poroes media: Theory, numerical model, and its verification. *Water Resources Research*, 26, 1990.

[29] D. Kavetski, P. Binning, and S. W. Sloan. Adaptive time stepping and error control in a mass conservative numerical solution of the mixed form of richards equation. *Advances in Water Resources*, 24(6):595–605, 2001.

[30] C. E. Kees and C. T. Miller. C++ implementations of numerical methods for solving differential-algebraic equations: Design and optimization considerations. *Association for Computing Machinery, Transactions on Mathematical Software*, 25(4):377–403, 1999.

[31] C. E. Kees and C. T. Miller. Higher order time integration methods for two-phase flow. *Advances in Water Resources*, 25(2):159–177, 2002.

[32] C. T. Kelley. *Iterative Methods for Linear and Nonlinear Equations*. Society for Industrial and Applied Mathematics, Philadelphia, 1995.

[33] M. R. Kirkland, R. G. Hills, and P. J. Wierenga. Algorithms for solving richards' equation for variably saturated soils. *Water Resources Research*, 28(8):2049–2058, 1992.

[34] J. B. Kool and J. C. Parker. Development and evaluation of closed-form expressions for hysteretic soil hydraulic properties. *Water Resources Research*, 23(1):105–114, 1987.

[35] C. T. Miller, G. A. Williams, C. T. Kelley, and M. D. Tocci. Robust solution of Richards' equation for non-uniform porous media. *Water Resources Research*, 34(10):2599–2610, 1998.

[36] P. C. D. Milly. A mass-conservative procedure for time-stepping in models of unsaturated flow. *Advances in Water Resources*, 8(3):32–36, 1985.

[37] Y. Mualem. A new model for predicting the hydraulic conductivity of unsaturated porous media. *Water Resources Research*, 12(3):513–522, 1976.

[38] J. T. Oden, I. Babuska, and C. E. Baumann. A discontinuous hp finite element method for diffusion problems. *Journal of Computaional Physics*, 146(2):491–519, 1998.

[39] H. S. Oh, J. K. Lim, and S. Y. Han. An rh-method for efficient adaptive finite element analysis. *Communications In Numerical Methods In Engineering*, 14(6):549–558, 1998.

[40] C. Paniconi, A. A. Aldama, and E. F. Wood. Numerical evaluation of interative and noniterative methods for the solution of the nonlinear richards equation. *Water Resources Research*, 27(6):1147–1163, 1991.

[41] D. W. Pepper and D. B. Carrington. Application of h-adaptation for environmental fluid flow and species transport. *International Journal for Numerical Methods in Fluids*, 31(1):275–183, 1999.

[42] K. Rathfelder and L. M. Abriola. Impact of grid resolution and parametric representation on multiphase flow simulations. In A. Peters, G. Wittum, B. Herrling, U. Meissner, C. A. Brebbia, W. G. Gray, and G. F. Pinder, editors, *Computational Methods in Water Resources X*, volume Vol. 2, pages 983–990, Dordrecht, The Netherlands, 1994. Kluwer Academic Publishers.

[43] J. W. Reeder. Infiltration under rapidly varying surface water depths. *Water Resources Research*, 16(1):97–104, 1980.

[44] P. J. Ross. Efficient numerical methods for infiltration using Richards' equation. *Water Resources Research*, 26(2):279–290, 1990.

[45] P. Saucez, A. V. Wouver, and W. E. Scheisser. An adaptive method of lines solution of the korteweg-de vries equation. *Computers and Mathematics with Applications*, 35(12):13–25, 1998.

[46] W. E. Schiesser. Method of lines solution of the korteweg-de vries equation. *Computers and Mathematics with Applications*, 28(10-12):147–154, 1994.

[47] L. Tang and J. D. Baeder. Uniformly accurate finite difference schemes for p-refinement. *SIAM Journal on Scientific Computing*, 20(3):1115–1131, 1999.

[48] M. D. Tocci, C. T. Kelley, and C. T. Miller. Accurate and economical solution of the pressure-head form of Richards' equation by the method of lines. *Advances in Water Resources*, 20(1):1–14, 1997.

[49] M. D. Tocci, C. T. Kelley, C. T. Miller, and C. E. Kees. Inexact Newton methods and the method of lines for solving Richards' equation in two space dimensions. *Computational Geosciences*, 2(4):291–309, 1999.

[50] A. S. Usmani. Solution of steady and transient advection problems using an h-adaptive finite element method. *International Journal of Computational Fluid Dynamics*, 11(3-4):249–259, 1999.

[51] M. Th. van Genuchten. A closed-form equation for predicting the hydraulic conductivity of unsaturated soils. *Soil Science Society of America Journal*, 44:892–898, 1980.

[52] A. W. Warrick, G. J. Mullen, and D. R. Nielsen. Scaling field-measured soil hydraulic properties using a similar media concept. *Water Resources Research*, 13(2):355–362, 1977.

[53] G. A. Williams and C. T. Miller. An evaluation of temporally adaptive transformation approaches for solving Richards' equation. *Advances in Water Resources*, 22(8):831–840, 1999.